J|A|C|S ARTICLES

Published on Web 05/21/2009

Kinetic, Structural, and EPR Studies Reveal That Aldehyde Oxidoreductase from *Desulfovibrio gigas* Does Not Need a Sulfido Ligand for Catalysis and Give Evidence for a Direct Mo−C Interaction in a Biological System

Teresa Santos-Silva,[†] Felix Ferroni,[‡] Anders Thapper,[†,§] Jacopo Marangon,[†] Pablo J. González,[†] Alberto C. Rizzi,[‡] Isabel Moura,[†] José J. G. Moura,*[,†] Maria J. Romão,*[,†] and Carlos D. Brondino*[,‡]

REQUIMTE, Departamento de Química, Centro de Química Fina e Biotecnologia, Faculdade de Ciências e Tecnologia, Universidade Nova de Lisboa, 2829-516 Caparica, Portugal, and Departamento de Física, Facultad de Bioquímica y Ciencias Biológicas, Universidad Nacional del Litoral, 3000ZAA Santa Fe, Argentina

Received December 3, 2008; E-mail: jose.moura@dq.fct.unl.pt; mromao@dq.fct.unl.pt; brondino@fbcb.unl.edu.ar

Abstract: Aldehyde oxidoreductase from *Desulfovibrio gigas* (*Dg*AOR) is a member of the xanthine oxidase (XO) family of mononuclear Mo-enzymes that catalyzes the oxidation of aldehydes to carboxylic acids. The molybdenum site in the enzymes of the XO family shows a distorted square pyramidal geometry in which two ligands, a hydroxyl/water molecule (the catalytic labile site) and a sulfido ligand, have been shown to be essential for catalysis. We report here steady-state kinetic studies of *Dg*AOR with the inhibitors cyanide, ethylene glycol, glycerol, and arsenite, together with crystallographic and EPR studies of the enzyme after reaction with the two alcohols. In contrast to what has been observed in other members of the XO family, cyanide, ethylene glycol, and glycerol are reversible inhibitors of *Dg*AOR. Kinetic data with both cyanide and samples prepared from single crystals confirm that *Dg*AOR does not need a sulfido ligand for catalysis and confirm the absence of this ligand in the coordination sphere of the molybdenum atom in the active enzyme. Addition of ethylene glycol and glycerol to dithionite-reduced *Dg*AOR yields rhombic Mo(V) EPR signals, suggesting that the nearly square pyramidal coordination of the active enzyme is distorted upon alcohol inhibition. This is in agreement with the X-ray structure of the ethylene glycol and glycerol-inhibited enzyme, where the catalytically labile OH/OH_2 ligand is lost and both alcohols coordinate the Mo site in a η^2 fashion. The two adducts present a direct interaction between the molybdenum and one of the carbon atoms of the alcohol moiety, which constitutes the first structural evidence for such a bond in a biological system.

Introduction

The enzymes of the xanthine oxidase (XO) family are a distinct type of protein that contains molybdenum in a mononuclear form in the active site. The enzymes of this family generally catalyze hydroxylation reactions where, unlike other hydroxylases, water rather than dioxygen is the source of the oxygen atom that is inserted into substrate.[1,2]

The active site in the enzymes of the XO has been extensively characterized and it has been shown that the Mo atom in its oxidized form is in a distorted square pyramidal coordination with two S atoms from one pyranopterin, a sulfido ligand and a OH/OH_2 molecule in equatorial positions, and an oxo ligand in the apical position (Figure 1a).[3−5] The OH/OH_2 ligand (hereafter the OH_x ligand) occupies the catalytic labile site of the protein, where substrate and inhibitors such as arsenite bind the molybdenum atom.[6−9] The sulfido ligand is essential for catalysis and can be removed by cyanide treatment to give the inactive desulfo form of the enzyme (Figure 1b).[10] The currently most accepted reaction mechanism implies a base-assisted nucleophilic attack on the carbon atom to be hydroxylated by the OH_x ligand and concomitant hydride transfer to the sulfido

[†] Universidade Nova de Lisboa.
[‡] Universidad Nacional del Litoral.
[§] Present address: Department of Photochemistry and Molecular Science, Uppsala University, P.O. Box 523, S-751 20 Uppsala, Sweden.

(1) Hille, R. *Chem. Rev.* **1996**, *96*, 2757–2816.
(2) Romao, M. J.; Cunha, C. A.; Brondino, C. D.; Moura, J. J. *Met. Ions Biol. Syst.* **2002**, *39*, 539–370.
(3) Brondino, C. D.; Romao, M. J.; Moura, I.; Moura, J. J. *Curr. Opin. Chem. Biol.* **2006**, *10*, 109–114.
(4) Hille, R. *Arch. Biochem. Biophys.* **2005**, *433*, 107–116.
(5) Hille, R. *Eur. J. Inorg. Chem.* **2006**, *2006*, 1913–1926.
(6) Okamoto, K.; Matsumoto, K.; Hille, R.; Eger, B. T.; Pai, E. F.; Nishino, T. *Proc. Natl. Acad. Sci. U.S.A.* **2004**, *101*, 7931–7936.
(7) Boer, D. R.; Thapper, A.; Brondino, C. D.; Romao, M. J.; Moura, J. J. *J. Am. Chem. Soc.* **2004**, *126*, 8614–8615.
(8) Thapper, A.; Boer, D. R.; Brondino, C. D.; Moura, J. J.; Romao, M. J. *J. Biol. Inorg. Chem.* **2007**, *12*, 353–366.
(9) Truglio, J. J.; Theis, K.; Leimkuhler, S.; Rappa, R.; Rajagopalan, K. V.; Kisker, C. *Structure* **2002**, *10*, 115–125.
(10) Massey, V.; Edmondson, D. *J. Biol. Chem.* **1970**, *245*, 6595–6598.

 10.1021/ja809448r CCC: $40.75

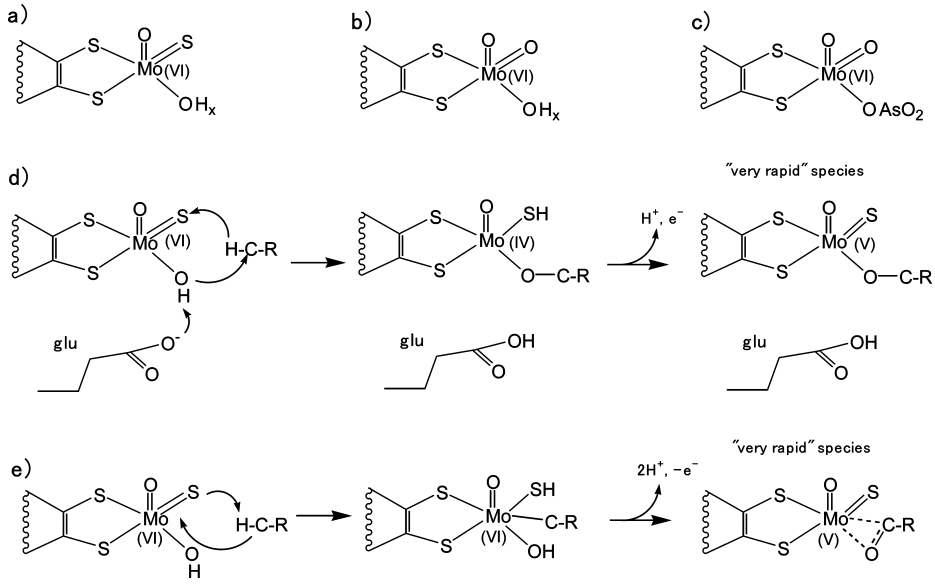

Figure 1. Top: Coordination around the molybdenum atom for the XO family of enzymes: (a) active form, (b) inactive desulfo form, and (c) structure of arsenite-inhibited *Dg*AOR. Middle and bottom: Mechanisms suggested for the active site−substrate interaction in the XO family, including the proposed structures for the paramagnetic "very rapid" species. (d) Base-assisted nucleophilic attack mechanism.[6,13] (e) Electrophilic attack mechanism as suggested by Howes et al. on the basis of ENDOR studies.[14]

ligand,[6,11−13] where the nearby glutamic acid residue acts as base for the proton of the OH_x ligand, enhancing its nucleophilic character. Structures of the most relevant intermediates of this proposal are given in Figure 1d. Howes et al. have proposed a rather different mechanism from ENDOR studies on the paramagnetic catalytic intermediate called "very rapid" (Figure 1e).[14] It involves addition of the substrate CH group across the Mo═S bond, a reaction with chemical precedent,[15] and simultaneous proton abstraction by the sulfido ligand. This reaction is proposed to be initiated through an electrophilic attack by Mo on the substrate C atom and attack by the OH_x ligand to give the product of the reaction (a C═O group) coordinated to Mo in a η^2 fashion. This proposal was later criticized by Manikandan et al., whose analysis of the ENDOR data does not support the existence of a direct Mo−C bond in the "very rapid species", thus favoring the first mechanism.[16]

Aldehyde oxidoreductases (AOR) from sulfate-reducing bacteria (SRB) are members of the XO family of mononuclear Mo-enzymes that catalyze the two-electron oxidation of aldehydes to their respective carboxylic acids. The 3D structure of AOR from *Desulfovibrio gigas* (*Dg*AOR) was the first crystallographic structure reported for a member of this family[17] and the first to be structurally characterized at near atomic resolution (1.28 Å) (the term native structure will be used to refer to this structure).[18] In contrast to xanthine oxidoreductase[6] and quinoline 2-oxidoreductase,[19] there is no structural evidence supporting the presence of a sulfido ligand coordinated to the Mo atom in active forms of AORs from SRB. However, its presence was suggested from spectroscopic studies, mainly electron paramagnetic resonance (EPR), since *Dg*AOR shows the typical Mo(V) EPR signals detected in the XO family of enzymes. The "rapid"-type Mo(V) EPR signals associated with the presence of the sulfido ligand were observed in AOR from the *Desulfovibrio* genus.[20] In addition, the Mo(V) EPR signals associated with desulfo forms of XO, such as the "slow"-type signal and the signal obtained upon ethylene glycol (EDO) addition, were also observed.[20−23] On this basis, it was assumed that AORs from SRB and XO family enzymes have similar active sites and that both would experience the same changes upon reaction with substrates, inhibitors, and reducing agents. Because the structural data of *Dg*AOR did not show the sulfido ligand coordinated to Mo, it was assumed that the enzyme crystallizes in the desulfo inactive form (Figure 1b).[17,18] A similar conclusion was obtained for the XO family member 4-hydroxybenzoyl-CoA-reductase (4-HBCR), for which structural data do not show evidence for the sulfido ligand,[24] although its presence was suggested by kinetic and spectroscopic data.[25] Studies on desulfo forms of distinct XO family members showed that the cyano-

(11) Huber, R.; Hof, P.; Duarte, R. O.; Moura, J. J.; Moura, I.; Liu, M. Y.; LeGall, J.; Hille, R.; Archer, M.; Romao, M. J. *Proc. Natl. Acad. Sci. U.S.A.* **1996**, *93*, 8846–8851.
(12) Nishino, T.; Okamoto, K.; Eger, B. T.; Pai, E. F.; Nishino, T. *FEBS J.* **2008**, *275*, 3278–3289.
(13) Pauff, J. M.; Zhang, J.; Bell, C. E.; Hille, R. *J. Biol. Chem.* **2008**, *283*, 4818–4824.
(14) Howes, B. D.; Bray, R. C.; Richards, R. L.; Turner, N. A.; Bennett, B.; Lowe, D. J. *Biochemistry* **1996**, *35*, 1432–1443.
(15) Coucouvanis, D.; Toupadakis, A.; Lane, J. D.; Koo, S. M.; Kim, C. G.; Hadjikyriacou, A. *J. Am. Chem. Soc.* **1991**, *113*, 5271–5282.
(16) Manikandan, P.; Choi, E. Y.; Hille, R.; Hoffman, B. M. *J. Am. Chem. Soc.* **2001**, *123*, 2658–2663.
(17) Romao, M. J.; Archer, M.; Moura, I.; Moura, J. J.; LeGall, J.; Engh, R.; Schneider, M.; Hof, P.; Huber, R. *Science* **1995**, *270*, 1170–1176.
(18) Rebelo, J. M.; Dias, J. M.; Huber, R.; Moura, J. J.; Romao, M. J. *J. Biol. Inorg. Chem.* **2001**, *6*, 791–800.
(19) Bonin, I.; Martins, B. M.; Purvanov, V.; Fetzner, S.; Huber, R.; Dobbek, H. *Structure* **2004**, *12*, 1425–1435.
(20) Turner, N.; Barata, B.; Bray, R. C.; Deistung, J.; Le Gall, J.; Moura, J. J. *Biochem. J.* **1987**, *243*, 755–761.
(21) Andrade, S. L.; Brondino, C. D.; Feio, M. J.; Moura, I.; Moura, J. J. *Eur. J. Biochem.* **2000**, *267*, 2054–2061.
(22) Duarte, R. O.; Archer, M.; Dias, J. M.; Bursakov, S.; Huber, R.; Moura, I.; Romao, M. J.; Moura, J. J. *Biochem. Biophys. Res. Commun.* **2000**, *268*, 745–749.
(23) Thapper, A.; Rivas, M. G.; Brondino, C. D.; Ollivier, B.; Fauque, G.; Moura, I.; Moura, J. J. *J. Inorg. Biochem.* **2006**, *100*, 44–50.
(24) Unciuleac, M.; Warkentin, E.; Page, C. C.; Boll, M.; Ermler, U. *Structure* **2004**, *12*, 2249–2256.
(25) Johannes, J.; Unciuleac, M. C.; Friedrich, T.; Warkentin, E.; Ermler, U.; Boll, M. *Biochemistry* **2008**, *47*, 4964–4972.

lyzable sulfido ligand can be reinserted with regain of the enzyme activity.[26] A crystallographic structure of "resulfurated" *Dg*AOR showed that a sulfido ligand can be introduced by soaking native crystals with sulfide ions.[11] However, in contrast to that observed in xanthine oxidoreductase[6] and quinoline 2-oxidoreductase,[19] the sulfido ligand was found in the apical position of the molybdenum site,[11] suggesting that the inclusion of the sulfur atom in *Dg*AOR might be the consequence of an unspecific reaction caused by the resulfuration conditions.

As reported elsewhere, several inhibitory agents of the XO family of enzymes such as arsenite, ethylene glycol, and glycerol (GOL) interact directly with the molybdenum site to yield stable Mo(V) complexes.[7,8,23,27] These inhibited forms are important to understand changes in the coordination of the active site and the integrity of the electron transfer chain upon inhibition. In previous structural and EPR studies of arsenite-inhibited *Dg*AOR, a correlation between structural and EPR properties of the Mo center was established.[7,8] The major findings of these studies were to elucidate the interaction between the inhibitory arsenite ion and the molybdenum atom (Figure 1c) and to establish that the sulfido ligand is not essential to determine the EPR properties of the arsenic-bound molybdenum center. Particularly, the latter raised some doubts about the presence of the sulfido ligand in active *Dg*AOR.

In this paper, we report steady-state kinetic, X-ray crystallographic, and EPR studies of *Dg*AOR. The kinetic studies were carried out with cyanide, EDO, GOL, and arsenite in order to compare the behavior of *Dg*AOR and XO toward these inhibitor agents. X-ray crystallographic and EPR studies of GOL- and EDO-inhibited *Dg*AOR were performed to understand the mode of interaction of the alcohol molecule on inhibition. Analysis of all these results contributes to a better understanding of the interaction mechanism between the enzyme and the different inhibitor molecules and to establish whether the sulfido ligand is present in the coordination sphere of the Mo atom of *Dg*AOR.

Experimental Section

Protein Purification and Quantification. *Dg*AOR was purified as described elsewhere.[28,29] Protein quantification was performed using either the Bradford method[30] with bovine serum albumin as standard or using the molar absorption coefficient at 462 nm (ε = 24.6 mM^{-1} cm^{-1}).

Enzyme Kinetic Assays. Steady-state kinetic studies of *Dg*AOR were performed aerobically at 310 K by measuring the rate of 2,6-dichlorophenol−indophenol (DCPIP) reduction at 600 nm (ε = 21 mM^{-1} cm^{-1}) in a 1 cm optical path length cell containing the following reaction mixture: 50 mM Tris-HCl buffer (pH 7.6), 35 μM DCPIP, 500 nM enzyme, and benzaldehyde as substrate. Concentrations of 5−200 μM benzaldehyde were assayed and initial rates were obtained for the determination of kinetic constants. In all assays, the substrate was the last component to be added, after 5 min equilibration of the protein with the electron acceptor. Under these experimental conditions, one enzymatic unit (U) corresponds to 1 μmol of benzaldehyde oxidized per min and the specific activity is U/mg of enzyme.

Inhibition assays toward different agents followed by dialysis were performed to evaluate reversibility. Samples of 30 μM *Dg*AOR were incubated for 2 h at room temperature with 50 mM potasium cyanide, 1 mM EDO, 1 mM GOL, and 24 μM sodium arsenite, respectively, all in 100 mM Tris-HCl buffer, pH 7.6. At these inhibitor concentrations and after 10 min incubation, inhibition is significantly detected. After 2 h incubation, the inhibitors were separated from the enzyme samples by ultrafiltration (Centricon Ultra 30 K) (five dilution−concentration cycles), and the activity was measured again. As-prepared *Dg*AOR was used as a control. The same procedure was applied to bovine milk xanthine oxidase purchased from Sigma (reference X4500) and cyanide using the kinetic assay described for *Dg*AOR but replacing benzaldehyde for xanthine.

Kinetic studies of reversible inhibition reactions were performed as for the as-prepared enzyme. The reaction mixtures were set as described above and the reaction was started adding the inhibitor and the substrate simultaneously using the concentrations reported in the Supporting Information. Enzyme kinetic constants were determined as explained in refs 31 and 32.

Sample Preparation for EPR Spectroscopy. EDO- and GOL-Inhibited Samples. As-prepared *Dg*AOR samples (200 μM in 10 mM Tris-HCl buffer pH 7.6) were reduced for 20 min under argon atmosphere using a 50-fold molar excess of sodium dithionite to yield the "slow" EPR signal.[29] Then, a large excess of the inhibitor (1 M) was added to the fully reduced sample still under an argon atmosphere. Finally, the sample was incubated for 4 h at 4 °C. EDO- and GOL-inhibited *Dg*AOR samples were set as described above using both H_2O- and D_2O-based buffers (pD was corrected using a DCl solution). Reoxidation of these inhibited samples was performed by exposure to air at 4 °C until no EPR signals from the [2Fe-2S] centers could be observed at low temperatures.

Cyanide-Inhibited Samples. As-prepared *Dg*AOR (200 μM in 10 mM Tris-HCl buffer pH 7.6) were incubated with 10 mM cyanide for 10 min at 4 °C and then reduced with dithionite for 20 min at 4 °C. In a parallel assay, cyanide in the same concentration was added to a *Dg*AOR sample showing the slow-type signal obtained as described above.

Experimental and Computer-Simulated EPR spectra. EPR spectra were recorded on a Bruker EMX spectrometer equipped with a rectangular cavity (model ER 4102ST) and an Oxford Instruments continuous flow cryostat. Spectra were recorded between 20 and 140 K at 9.5 GHz. The microwave power used was 2 mW at temperatures of 100 K or above and 0.06 mW below 100 K. The 100 kHz modulation amplitude was 2 G. Computer simulations of the spectra were performed using the program WIN-EPR Simfonia.

Crystallization and Soaking Procedures. *Dg*AOR was crystallized as described before using the sitting-drop vapor-diffusion method.[33] Crystallization drops were prepared by adding 4 μL of protein at 10 mg/mL in 10 mM Tris-HCl buffer (pH 7.6) to 2 μL of precipitating solution containing 30% 2-propanol, 0.2 M magnesium chloride, and 0.2 M HEPES buffer (pH 7.6). Dark red, ruby-shaped crystals grew to their maximum size of 0.3 × 0.2 × 0.2 mm in 2−3 weeks at 4 °C. In order to stabilize the crystals, a solution of a harvesting buffer (HB1) containing 30% (w/v) polyethylene glycol 4000, 30% 2-propanol, 0.2 M magnesium chloride, and 0.2 M HEPES buffer was prepared. HB1 was slowly added to the crystal drops for at least 48 h. Since one of the aims of this study was to analyze the interaction of ethylene glycol and glycerol with the active site, 2-propanol, present in the active site of the native structure, had to be removed. Hence, a second harvesting buffer (HB2) was prepared with no 2-propanol, containing 30% (w/v) polyethylene glycol 4000, 0.2 M magnesium chloride, and 0.2 M HEPES buffer. HB2 was carefully added to

(26) Wahl, R. C.; Rajagopalan, K. V. *J. Biol. Chem.* **1982**, *257*, 1354–1359.
(27) Lowe, D. J.; Barber, M. J.; Pawlik, R. T.; Bray, R. C. *Biochem. J.* **1976**, *155*, 81–85.
(28) Moura, J. J.; Xavier, A. V.; Bruschi, M.; Le Gall, J.; Hall, D. O.; Cammack, R. *Biochem. Biophys. Res. Commun.* **1976**, *72*, 782–789.
(29) Moura, J. J.; Xavier, A. V.; Cammack, R.; Hall, D. O.; Bruschi, M.; Le Gall, J. *Biochem. J.* **1978**, *173*, 419–425.
(30) Bradford, M. M. *Anal. Biochem.* **1976**, *72*, 248–54.
(32) Eisenthal, R.; Cornish-Bowden, A. *Biochem. J.* **1974**, *139*, 715–720.
(31) Cornish-Bowden, A.; Eisenthal, R. *Biochem. J.* **1974**, *139*, 721–730.
(33) Romao, M. J.; Barata, B. A.; Archer, M.; Lobeck, K.; Moura, I.; Carrondo, M. A.; LeGall, J.; Lottspeich, F.; Huber, R.; Moura, J. J. *Eur. J. Biochem.* **1993**, *215*, 729–732.

Table 1. Data Collection Statistics[a]

crystal	ethylene glycol (EDO)	glycerol (GOL)
space group	$P6_122$	$P6_122$
unit cell (Å)	*a, b* = 142.80, *c* = 161.55	*a, b* = 142.56, *c* = 161.88
Mathews parameter (Å^3/Da)	2.43	2.43
data collection statistics		
wavelength (Å)	0.931 00	0.931 00
no. observed reflections	390 564	402 976
no. unique reflections	89 511 (45 045)	101 724 (14 763)
resolution limits (Å)	30.37−1.79 (1.89−1.79)	28.92−1.72 (1.81−1.72)
completeness (%)	98.4 (97.5)	99.2 (99.2)
redundancy	4.4 (3.5)	4.0 (3.9)
average $I/\sigma(I)$	16.7 (3.5)	10.7 (2.3)
R_{sym} (%)	6.2 (32.7)	8.6 (44.6)

[a] Values in parentheses correspond to data in the outermost shell.

Table 2. Refinement Statistics

refinement statistics	ethylene glycol (EDO)	glycerol (GOL)
resolution limits (Å)	30.37−1.79	28.92−1.72
R-factor (%)	15.3	16.0
no. of reflections	96547	85025
R-free (%)	18.9	19.1
no. of reflections	4817	4242
no. residues	907	907
no. atoms	8163	8094
no. residues missing	0	0
rmsd bond length (Å)	0.012	0.013
rmsd bond angles (deg)	1.420	1.461
average temperature factor (Å^2)		
main chain atoms	17.137	24.698
side chain atoms	18.367	25.961
water molecules	32.629	31.534
Ramachandran plot (%)		
residues in most favored regions	91.7	91.7
residues in additionally allowed regions	7.6	7.6
residues in generously allowed regions	0.3	0.4
residues in disallowed regions	0.4	0.3
overall *G*-factor	0.07	0.07

the drops in order to replace the precipitating solution and HB1. After 3 days, crystals were transferred to a new drop of HB2 alone.

Stabilized and 2-propanol free *Dg*AOR crystals were soaked with a third harvesting buffer solution containing either EDO (HB3EDO) or GOL (HB3GOL). HB3EDO was prepared with 30% (w/v) polyethylene glycol 4000, 0.2 M magnesium chloride, 0.2 M HEPES buffer, and 40% (w/v) EDO, while HB3GOL was prepared by addition of 50% (w/v) GOL to HB2 to a final concentration of 10% (w/v). In both cases, crystals were left in these solutions for 3−4 days and flash frozen for data collection.

Data Collection, Structure Determination, and Refinement. Two data sets of the flash-frozen soaked crystals were collected at ID14-3 of the European Synchrotron Radiation Facility (ESRF, Grenoble, France), one for the EDO soak (EDO data set) and a second for the GOL soak (GOL data set). The crystals diffract to beyond 1.8 Å resolution and belong to the same space group as the native crystals, with similar cell constants. MOSFLM[34] and SCALA[35] from the CCP4 suite[36] were used to process the data, which are summarized in Table 1.

Structure determination was performed with PHASER,[37] using the molecular model obtained at 1.28 Å resolution (PDB accession code 1VLB).[18,38] A density modification protocol was applied using DM,[39] giving good initial phases with ca. 0.7 mean figure of merit and 50% solvent content. Restrained refinement was performed with REFMAC 5.2,[40] and the ligands of the molybdenum atom were not included in the initial cycles. Inspection of the electron density maps using COOT[41] and repeated cycles of refinement allowed identification in each structure of the alcohols, EDO and GOL, respectively, coordinated to the metal ion. COOT was also used to generate water molecules, most of these in accordance with the 1VLB structural model.

In the last stages of refinement, temperature factors were refined anisotropically for the molybdenum, iron, sulfur from the two [2Fe-2S] clusters, chloride, and magnesium atoms and isotropically for the remaining protein and solvent atoms. In both data sets, R-work and R-free converged to approximately 15% and 19%, respectively, and geometrical validation was carried out by several programs such as PROCHECK,[42] STAN,[43] and MOLPROBITY.[44] Analysis of the Ramachandran plot showed that 99.3% of the protein residues are in most favored or additionally allowed regions, while only a small fraction of residues, 0.7%, are in generously allowed or disallowed regions of the plot. Refinement statistics are summarized in Table 2. Coordinates and observed structure factor amplitudes of EDO- and GOL-inhibited forms of *Dg*AOR have been deposited in the Protein Data Bank under the accession codes 3FC4 and 3FAH, respectively.

Results

Kinetic Studies. The reaction of *Dg*AOR with benzaldehyde follows a Michaelis−Menten mechanism with kinetic parameters $K_M = 9.7 \pm 0.5$ μM, $V_{max} = 0.0337 \pm 0.0004$ μmol/min, and $k_{cat} = 1.12 \pm 0.01$ s^{-1} (Figure S1 in Supporting Information). Similar values were reported for other AORs from SRB with the same substrate.[21−23]

Kinetic assays followed by dialysis were performed to determine whether the inhibition with EDO, GOL, cyanide, and arsenite is reversible or not. At the indicated inhibitor concentrations after 10 min incubation, the percentages of remnant activity for each inhibitor were 78.1 ± 0.4 for EDO, 48 ± 3 for GOL, and 69.1 ± 0.1 for cyanide; no activity was detected for arsenite. It is important to note that the cyanide concentration used to inhibit *Dg*AOR is ∼10 times the concentration used to produce cyanolysis of the sulfido ligand in XO,[10] whereas the arsenite concentration was similar to that used in XO.[45,46] After dialysis, the arsenite-inhibited sample remains inactive, indicating that arsenite is an irreversible inhibitor. In contrast, the percentages of remnant activity of the EDO-, GOL-, and cyanide-treated samples are near to the control value, 98.8 ± 0.5, 94.0 ± 0.4, 99.5 ± 0.1, respectively, confirming the reversible behavior of these inhibitors. When the same protocol was applied to bovine milk xanthine oxidase and cyanide, no activity toward xanthine was detected after removal of the inhibitor, which confirms the efficiency of the method used to test the inactivation of *Dg*AOR.

(34) Leslie, A. G. W. In *Joint CCP4 and ESF-EACMB Newsletter on Protein Crystallography No. 26*, Daresbury Laboratory: Warrington, UK, 1992.
(35) Kabsch, W. *J. Appl. Crystallogr.* **1988**, *21*, 67–72.
(36) Collaborative Computational Project, Number 4, *Acta Crystallogr. Sect. D* **1994**, *50*, 760–763.
(37) Read, R. J. *Acta Crystallogr. Sect. D* **2001**, *57*, 1373–1382.
(38) Berman, H. M.; Westbrook, J.; Feng, Z.; Gilliland, G.; Bhat, T. N.; Weissig, H.; Shindyalov, I. N.; Bourne, P. E. *Nucleic Acids Res.* **2000**, *28*, 235–242.
(39) Cowtan, K. D.; Zhang, K. Y. *Prog. Biophys. Mol. Biol.* **1999**, *72*, 245–270.
(40) Murshudov, G. N.; Vagin, A. A.; Dodson, E. J. *Acta Crystallogr. Sect. D* **1997**, *53*, 240–255.
(41) Emsley, P.; Cowtan, K. *Acta Crystallogr. Sect. D.* **2004**, *60*, 2126–2132.
(42) Laskowski, R. A.; MacArthur, M. W.; Moss, D. S.; Thornton, J. M. *J. Appl. Crystallogr.* **1993**, *26*, 283–291.
(43) Nayal, M.; Di Cera, E. *J. Mol. Biol.* **1996**, *256*, 228–234.
(44) Davis, I. W.; Leaver-Fay, A.; Chen, V. B.; Block, J. N.; Kapral, G. J.; Wang, X.; Murray, L. W.; Arendall, W. B., 3rd; Snoeyink, J.; Richardson, J. S.; Richardson, D. C. *Nucleic Acids Res.* **2007**, *35*, W375–383.
(45) Hille, R.; Stewart, R. C.; Fee, J. A.; Massey, V. *J. Biol. Chem.* **1983**, *258*, 4849–4856.
(46) George, G. N.; Bray, R. C. *Biochemistry* **1983**, *22*, 1013–1021.

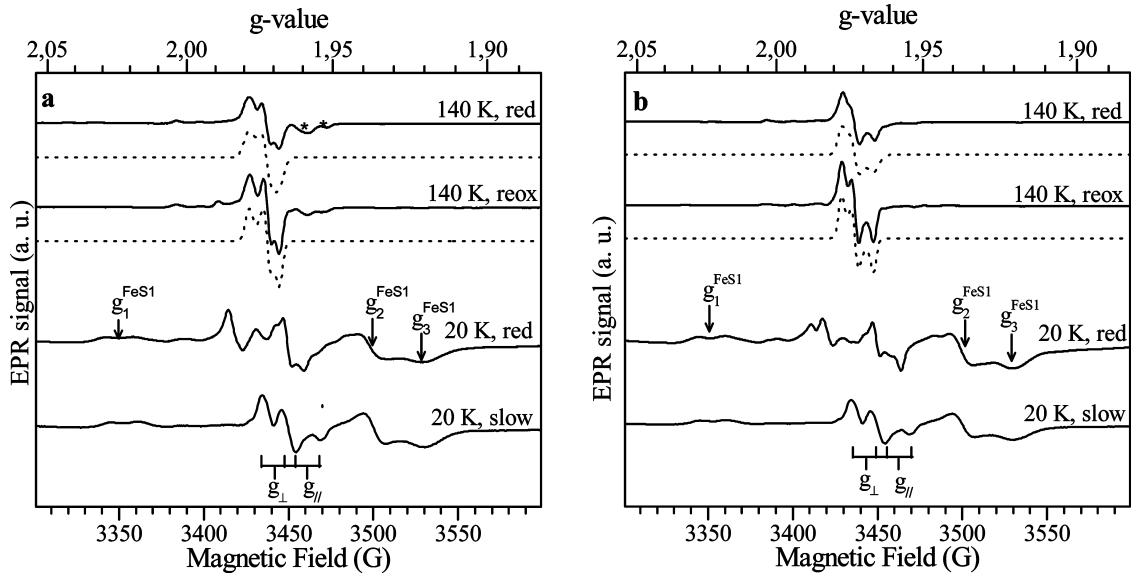

Figure 2. (a) EPR signals obtained after ethylene glycol addition to a dithionite-reduced *Dg*AOR sample (solid lines) and simulations (dash lines). The spectra labeled "red" correspond to a sample incubated for 4 h in anaerobic conditions, and the spectrum labeled "reox" is obtained after air exposure of the "red" sample. The asterisks indicate resonance lines from the slow-type signal. EPR parameters for simulation of the "reox" signal were $g_1 = 1.9785(4)$, $g_2 = 1.9723(4)$, and $g_3 = 1.9681(4)$. Line width in gauss in parentheses. The same g-values were used for the "red" signal, except the line widths (5.5, 5, 6 G). (b) As for part a but with glycerol. EPR parameters for simulation of the "reox" signal were $g_1 = 1.9774(4)$, $g_2 = 1.9728(4)$, and $g_3 = 1.9665(4)$. Line width in gauss in parentheses. Similar g-values were used for the "red" signal, except the line widths (4.5, 4.5, 6 G). The three g-values of the FeS1 EPR signal are indicated with arrows. The split slow-type EPR signal obtained in a D_2O-exchanged sample of *Dg*AOR is included for comparison ($g_1 \sim g_2 = g_\perp = 1.970$ and $g_{||} = 1.959$). The splitting of the $g_\perp$ and $g_{||}$ features is indicated on the figure.

The inhibition type of the three reversible inhibitor agents was also studied. Cyanide displays a competitive inhibition pattern (Figure S2, Supporting Information, $K_{iC} = 6.6$ mM). EDO shows a mixed inhibition pattern (Figure S3, Supporting Information, $K_{iC} = 1.9$ mM and $K_{iU} = 6.4$ mM) and GOL a competitive inhibition pattern (Figure S4, Supporting Information, $K_{iC} = 26.8$ mM).

The above-reported results show that compounds that irreversibly inactivate several proteins of the XO family do not have the same effect on *Dg*AOR. To determine if the crystallized desulfo form of *Dg*AOR is active toward benzaldehyde, kinetic studies of enzyme samples prepared from dissolved single crystals were performed. An as-isolated sample of *Dg*AOR, showing a specific activity of 2.1 U/mg, was crystallized as explained in the Experimental Section. Approximately 40 crystals of *Dg*AOR were dissolved in 10 mM Tris-HCl pH 7.6 and assayed for kinetic activity. The kinetic assay of this enzyme sample displays a specific activity of 2.8 U/mg, which is slightly higher than that of the original one due to the higher purity of the crystallized enzyme. This demonstrates that the crystallized form of *Dg*AOR, which has no sulfido ligand coordinated to the molybdenum atom,[18] is catalytically competent.

EPR Spectroscopy of *Dg*AOR Inhibited with Ethylene Glycol, Glycerol, and Cyanide. The EPR spectra of dithionite-reduced *Dg*AOR samples reacted with either EDO or GOL show EPR signals associated with the different metal cofactors of the enzyme, which can be distinguished from their different g-values and relaxation behavior. The spectra recorded at 140 K are associated with Mo(V) species (Figure 2), whereas the spectra recorded at lower temperatures show the typical signals associated with the two [2Fe-2S] clusters present in the structure of *Dg*AOR, in addition to the Mo(V) signals.[47]

The Mo(V) signals observed in *Dg*AOR with EDO and GOL show rhombic symmetry and similar g-values (spectra at 140 K in Figure 2, EPR parameters in the caption to the figure). During incubation, a mixture of the slow-type signal ($g_1 \sim g_2 = g_\perp = 1.970$ and $g_{||} = 1.959$) and the corresponding one for each alcohol-inhibited sample was observed (the larger the incubation time, the higher the ratio between the signal obtained on alcohol addition and the slow-type signal, not shown). Air exposure of these samples shows EPR signals with the same g-values but smaller line widths, indicating that the corresponding Mo(V) species are stable in the redox potential range of +50 mV (value obtained after air reoxidation) and −400 mV (value obtained for the dithionite-reduced sample followed by alcohol addition). Minor features observed in both spectra correspond to the hyperfine structure given by the nuclear spin of the ^{95}Mo and ^{97}Mo isotopes ($I = 5/2$, natural abundancy 15.90% and 9.60%, respectively) and to a small component corresponding to the slow-type signal, which was only detected in the sample reacted with EDO. The spectra obtained in D_2O-exchanged samples show g-values similar to those obtained in normal water and do not show hyperfine structure attributable to solvent exchangeable protons (not shown). Similar results were reported for milk XO.[27]

The spectra at 20 K in Figure 2 show, in addition to the Mo(V) signal, the EPR signals associated with the proximal (FeS1, $g_1 = 2.023$, $g_2 = 1.938$, $g_3 = 1.919$) and the distal (FeS2, $g_1 = 2.060$, $g_2 = 1.9979$, $g_3 = 1.900$) iron−sulfur centers present in the structure of *Dg*AOR.[17] These spectra have g-values and temperature dependence (not shown) similar to those observed in dithionite-reduced *Dg*AOR (and other AORs from SRB) and show the g_1 splitting associated with the magnetic coupling between FeS1 and FeS2 (the g_1 feature of the FeS1 signal shows a splitting of ∼16 G; see Figure 2).[3] This indicates that neither the structure nor the chemical paths connecting FeS centers are affected on inhibition. The spectra at 20 K show also that the Mo(V) signal is split by magnetic interaction with FeS1, as usually observed in the proteins belonging to the XO family. The splitting of the slow signal in AORs from SRB is nearly

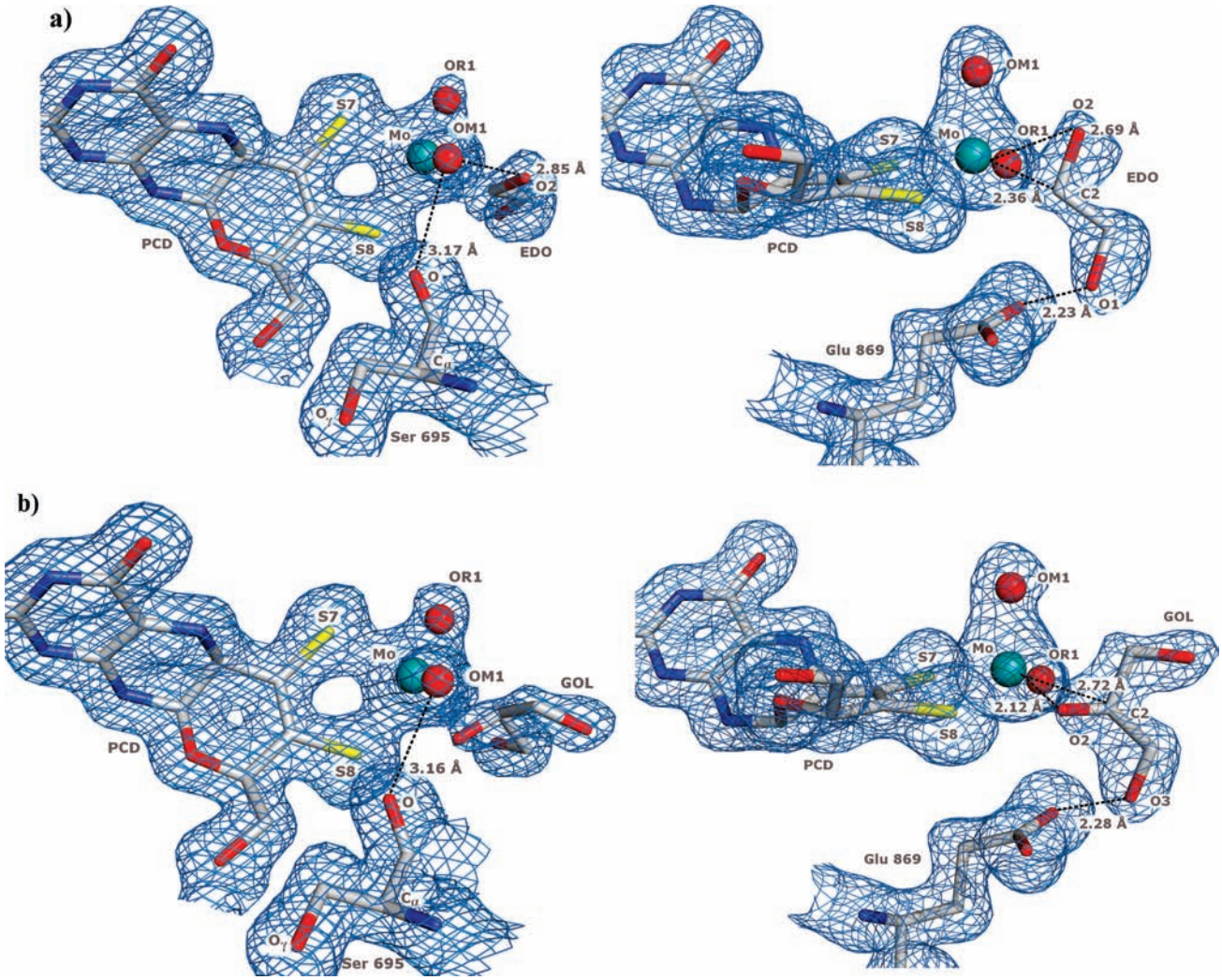

Figure 3. Structural representation of *Dg*AOR active site in a top and side view, soaked with (a) ethylene glycol (EDO) and (b) glycerol (GOL) and the $2F_o - F_c$ electron density map contoured at 1.0σ. Highlighted are the distances between the molybdenum and the oxygen and carbon atoms of the two alcohols together with selected hydrogen bonds in the vicinity of the Mo center. The EDO and the GOL molecules are occupying the position of the labile water/hydroxyl molecule, found in the native structure, and the distances between the metal and the ligands suggest a direct coordination. The pictures were prepared using Pymol software.[51]

isotropic, ca. 12 G (Figure 2).[3] The Mo(V) signal splitting of the alcohol-inhibited enzyme is more anisotropic (Figure 2, spectra at 20 K), but one can roughly estimate that the isotropic coupling is ~2 times larger than the one for the slow-type signal in both alcohol-inhibited samples. Magnetic couplings between two paramagnetic centers showing different relaxation times give temperature-dependent splitting of the resonance lines of the center relaxing slower.[48−50] For the case of the slow-type signal, the nearly isotropic splitting is completely averaged out at temperatures ~100 K or above [FeS1 relaxes faster than Mo(V)].[21−23] This is not the case of the alcohol-inhibited *Dg*AOR signals (Figure 2), which demonstrates that the larger line width of the "red" signals with respect to the "reox" signals at 140 K is due to the larger magnetic coupling between Mo(V) and FeS1 centers.

EPR spectra of cyanide-inhibited *Dg*AOR show no significant differences with those obtained from as-isolated samples in similar conditions (not shown). Dithionite reduction of cyanide-inhibited *Dg*AOR gives rise to a mixture of the "rapid-type 2" signal ($g_1 = 1.988$, $g_2 = 1.970$, $g_3 = 1.964$) and the "slow"-type signal right after reductant addition and only to the slow-type signal after 20 min incubation. Cyanide addition to dithionite-reduced *Dg*AOR does not modify either the line shape or intensity of the slow-type signal. This indicates that no enzyme−inhibitor interaction can be detected using EPR in these experimental conditions.

Table 3. Relevant Distances (in Å) from the Molybdenum Atom to Its Ligands in the Crystal Structures of EDO-Inhibited, GOL-Inhibited, and Native *Dg*AOR

	EDO (1.79 Å)[a]	GOL (1.72 Å)[a]	Native[18] (1.28 Å)[a]
Mo−OM1[b]	2.08	2.08	1.74
Mo−OR1[b]	1.75	1.75	1.79
Mo−S7[c]	2.32	2.34	2.41
Mo−S8[c]	2.39	2.41	2.49
Mo−O2[d]	2.69	2.12	
Mo−C2[d]	2.36	2.72	
Mo−OH$_x$			1.99

[a] Higher resolution limit of the X-ray data. [b] OM1 and OR1 correspond to hydroxo and oxo ligands, respectively, in the EDO- and GOL-inhibited structures and to oxo ligands in the native structure. [c] S7 and S8 are the sulfur atoms from the pyranopterin. [d] O2 and C2 are, respectively, the oxygen and carbon atoms belonging to the alcohol molecules.

Structural Data. The two AOR structures determined are very similar to each other as well as to the native structure[17,18] and

to the arsenite-inhibited form.[7,8] Structural superposition of these models has been done with the CCP4MG program (rmsd values of the superposition are given in Supporting Information, Table S1).

Regarding the protein structure, a few differences were observed in side chain positions and alternate conformations. A magnesium ion from the crystallization buffer, not identified previously in the native structure, was added to the two molecular models, as suggested by the STAN program.[43] This atom has a typical octahedral coordination to solvent molecules. The major differences between EDO and GOL structures, relative to the native structure, is the absence of the 2-propanol molecule, which was replaced by these molecules respectively, in similar positions at the active site (Figure 3).The absence of electron density for the 2-propanol proves that the soaking strategy to remove it from the crystallization solution was successful.

By examining the active site in detail, it is possible to identify in the experimental $2F_o - F_c$ maps of both alcohol-inhibited structures the molybdenum atom coordinated to the dithiolene sulfur atoms from the pterin moiety and to an oxo group (OR1), similar to the native structure (Table 3 and Figure 3). A hydroxo group (OM1H) at ca. 2.1 Å is replacing the apical oxo ligand found in the native structure. OM1H also establishes a hydrogen bond with the carbonyl oxygen atom of Ser 695. Furthermore, the distance between the dithiolene sulfur atoms (3.07 Å and 3.06 Å for EDO and GOL structures, respectively) also suggests that the Mo is partially reduced in both structures. This is in agreement with what has been described for studies with oxidized and reduced *Dg*AOR,[11] where the S−S distances were 3.5 and 3.0 Å in oxidized and reduced structures, respectively. In the $2F_o - F_c$ maps, and in the region where the OH_x ligand is found in the native structure, it was also possible to distinguish clear continuous electron density close to the metal atom in both structures, where a molecule of EDO and GOL, respectively, could be modeled. The distances between the metal and the surrounding atoms belonging to the two inhibitors are described in Table 3 and highly suggest a direct coordination to the Mo atom.

In the EDO structure, both C2 and O2 are involved in metal binding, at 2.4 and 2.7 Å from the molybdenum, respectively (Figure 3a). The hydroxyl group of the alcohol (O2H) is hydrogen bonded to the apical ligand of the metal center (OM1H). Atoms S7, S8, and OR1 of the Mo site and C2 of the glycol are approximately coplanar. The C2−O2H bond of the EDO molecule is nearly perpendicular to this plane (the angles O2−C2−S7, O2−C2−S8, and O2−C2−OR1 are ca. 100°, 110°, and 85°, respectively). The other hydroxyl group (O1H) of EDO is hydrogen bonded to the carboxylate group of the conserved and mechanistically relevant Glu 869.

In the GOL structure similar features are observed and, in the experimental $2F_o - F_c$ maps, clear electron density corresponding to the GOL molecule is evident (Figure 3b). However, GOL is bound to the metal atom in a different way than EDO. The C2 and O2 atoms of GOL are placed at 2.7 and 2.1 Å from Mo ion, respectively. The O2 atom coordinates the molybdenum in the position occupied by OH_x in the native structure. Another significant difference between the two inhibited structures is the orientation of the inhibitor in the active site. The C2−O2 bond from GOL is in the plane defined by atoms S7, S8, and OR1 of the Mo site. The GOL molecule is also involved in a hydrogen bond network. O2 is at 2.4 Å from the amino group of Gly 697 (not shown), while O3 is hydrogen bonded to Glu 869.

A chain of internal water molecules present in the native structure of *Dg*AOR is hydrogen bonded to the 2-propanol molecule.[17,18] These water molecules are also observed in the two structures now determined and establish hydrogen bonds to one of the hydroxyl groups of the inhibitors.

Discussion

The members of the XO family are closely related proteins that show a high degree of homology in their amino acid sequences, which is reflected in their overall structures, coordination around the metal centers, and EPR properties.[3,4] However, the fact that cyanide is a reversible inhibitor of *Dg*AOR constitutes a remarkable difference with respect to the other XO family members. Kinetic data obtained from cyanide-treated samples and samples prepared from single crystals confirm that *Dg*AOR does not need a sulfido ligand for catalysis, and hence the native structure corresponds to the enzyme active form.[17,18] This conclusion is reinforced by the data now reported of the inhibited forms. The dithionite-reduced desulfo forms of bovine milk XO after reaction with EDO show an EPR signal called "desulfo-inhibited" which is similar to those of the two alcohol-inhibited forms of *Dg*AOR (Figure 2).[27,52] This indicates that the Mo(V) species of *Dg*AOR giving rise to these EPR signals also correspond to desulfo forms. The fact that EDO and GOL are reversible inhibitors of *Dg*AOR is an additional proof that the sulfido ligand is not essential for catalysis in this enzyme. This finding implies that the role assigned to the sulfido group in XO, accepting the hydrogen attached to carbon of the substrate (either as a hydride or as a proton), should be accomplished by another Mo ligand in *Dg*AOR. The best candidate for this role is the equatorial oxo ligand (OR1) of the native enzyme. This hypothesis is based on EPR studies of arsenite-inhibited *Dg*AOR that showed that this oxo group is susceptible to protonation under reducing conditions.[8]

The steady-state kinetic studies of *Dg*AOR show that GOL is a competitive inhibitor, whereas EDO is a mixed inhibitor, although with a stronger competitive component. This is in line with the crystal structures of both alcohol-inhibited *Dg*AOR, which show the inhibitors covalently bound to the active site. The kinetic data also show that cyanide is a competitive inhibitor of *Dg*AOR. EPR experiments on cyanide-inhibited samples of *Dg*AOR are inconclusive on a plausible enzyme−inhibitor interaction. X-ray studies on crystals of *Dg*AOR soaked with cyanide would be necessary to understand the molecular basis of this inhibition process, but unfortunately, a suitable system for such study could not be obtained until now.

The crystallographic data reported here show that both alcohol inhibitor molecules bind the molybdenum atom, distorting the Mo center, which is in line with kinetic and EPR experiments. Kinetic data show undoubtedly that at high

(47) Bray, R. C.; Turner, N. A.; Le Gall, J.; Barata, B. A.; Moura, J. J. *Biochem. J.* **1991**, *280*, 817–820.
(48) More, C.; Asso, M.; Roger, G.; Guigliarelli, B.; Caldeira, J.; Moura, J.; Bertrand, P. *Biochemistry* **2005**, *44*, 11628–11635.
(49) Brondino, C. D.; Rivas, M. G.; Romao, M. J.; Moura, J. J.; Moura, I. *Acc. Chem. Res.* **2006**, *39*, 788–796.
(50) Caldeira, J.; Belle, V.; Asso, M.; Guigliarelli, B.; Moura, I.; Moura, J. J.; Bertrand, P. *Biochemistry* **2000**, *39*, 2700–2707.
(51) DeLano, W. L. *The PyMOL molecular graphics system*, Delano Scientific: San Carlos, CA, 2002.
(52) Edmondson, D. E.; D'Ardenne, S. C. *Biochemistry* **1989**, *28*, 5924–5930.

alcohol concentration the Mo−alcohol adducts are more stable than the square pyramidal complex of the native structure of *Dg*AOR. X-ray studies show that both alcohol molecules are stabilized in their respective positions by a hydrogen bond with the O atom from Glu869 (see Figure 3). A similar feature was also observed for the arsenite moiety in the structure of arsenite-inhibited *Dg*AOR[7,8] and for substrates in closely related proteins.[5,13] Additional proof of the stability of the Mo−alcohol adducts is given by the fact that inhibitor molecules cannot be easily removed once they entered into the active site pocket, as indicated by the extensive washing necessary for the enzyme to regain activity. The fact that the EPR signals obtained with both alcohols depart considerably from the axial symmetry associated with Mo(V) complexes in square pyramidal coordination indicates distorted molybdenum sites for both alcohol-inhibited species. The paramagnetic Mo(V) species produced with EDO and GOL are obtained from a dithionite-reduced form of *Dg*AOR followed by inhibitor addition. In contrast, the crystal structures now reported are obtained by reacting crystallized as-prepared enzyme with the inhibitor, which is assumed to have the Mo ion in the oxidized form. This indicates that either oxidized Mo(VI) or reduced Mo(IV) forms can react with the alcohol molecules, similar to what occurs for arsenite inhibition.[8] ENDOR studies of normal and deuterated EDO-treated XO detected a hyperfine coupling of 3.6 MHz (∼1.2 G) that was assigned to the protons of the CH_2 groups, confirming that the ethylene glycol is coordinated to Mo in the EPR-active species.[52] On the basis of this result, it was suggested that the Mo(V) ion is coordinated through both oxygen atoms of the alcohol moiety. Whether or not the EPR-active species presents a structure similar to those obtained by X-ray cannot be confirmed with the present data. X-ray structural determination of the EPR-active species would be necessary to elucidate this point.

Another remarkable feature of the EDO- and GOL-inhibited *Dg*AOR is the larger magnetic coupling between FeS1 and Mo(V) when compared to dithionite-reduced *Dg*AOR showing a slow-type signal. Magnetic coupling between two paramagnetic centers with $S = 1/2$ and dissimilar g-values can be produced by superexchange interaction, anisotropic and antisymmetric exchange, and dipolar coupling.[53] The first interaction yields an isotropic splitting of the resonance lines when $|J| < \Delta g\beta B$, where J is the exchange interaction constant, Δg is the difference between the effective g-factors of the interacting centers, β is the Bohr magneton, and B is the external magnetic field, whereas the other three interactions give anisotropic splitting. As also previously noted in milk XO,[27] the major contribution to the splitting of the Mo(V) signals is isotropic, indicating that the through-bond-mediated superexchange interaction is the dominant one. As EDO- and GOL-inhibited structures do not show changes with respect to the native structure of neither the chemical paths connecting FeS1 and Mo nor the orientation of the FeS1 center, the only cause for the larger splitting of the EPR signal is a reorientation of the Mo(V) magnetic orbital upon inhibition to favor the magnetic interaction between both centers.

The chemical form of the alcohol ligands in the EDO- and GOL-inhibited structures can only be speculated from comparisons with other well-established structures. The electron density map suggests a sp^3 hybrid orbital on C atoms of GOL, but there is not enough information to determine the hybridization type of the orbital on the C atoms of EDO. For the GOL-inhibited *Dg*AOR, the interaction with the Mo atom is mainly through the O2 atom of GOL. The distance Mo−O2 of 2.1 Å is in the range of what has been described for a Mo−O−R bond in model compounds (e.g., $[MoO_2\{O_2CC(S)Ph_2\}_2]^{2-}$, where the Mo−O distances are 2.174 and 2.176 Å).[54] The Mo−C2 distance of 2.7 Å is larger than the typical Mo−C distances reported in model compounds (2.0−2.5 Å). However, it may be considered as a weak bond.

A different situation is observed for the EDO-inhibited structure, in which the continuous electron density between protein and inhibitor highly suggests direct binding between Mo and the C2 atom of the alcohol moiety. There are molybdenum organometallic model complexes that show similar values for this bond (e.g., 2.352 Å for $[MoW(\mu\text{-}PPh_2)\{\mu\text{-}C(OH)C(C_6H_4Me\text{-}4)\}(CO)(\eta^7\text{-}C_7H_7)(\eta^5\text{-}C_2B_9H_{11})]$).[55] The structural data suggest that the reaction between Mo and EDO implies a process similar to that proposed in the reaction mechanism (see Introduction and Figure 1), which would imply that one of the protons attached to the C2 atom is lost upon inhibition. However, the possibility that the interaction Mo−EDO is mediated by an agostic interaction cannot be excluded, i.e. a three-center−two-electron Mo−H−C interaction, in which the electron density given to the Mo atom is given by the C−H bond.[56] As said above, the present quality of the electron density maps does not allow a clear identification of the chemical form of the alcohol molecule, and additional crystallographic and/or spectroscopic studies would be therefore necessary in order to unambiguously determine the binding modes of EDO in *Dg*AOR. Interestingly, the structure of the Mo−EDO complex resembles in some way that proposed by Bray and Lowe for the paramagnetic "very rapid" intermediate of the reaction (Figure 1e).[14] Although the present data can be taken neither as a confirmatory evidence of such a hypothesis nor an evidence against the base-assisted nucleophilic attack mechanism, they confirm that complexes showing a direct Mo−C interaction can be obtained under conditions of reversible inhibition. Hence, the formation of similar structures cannot be discarded as possible intermediates of the reaction.

Conclusions

The present kinetic data prove that *Dg*AOR is a member of the XO family of enzymes that catalyzes aldehyde oxidation without a sulfido ligand coordinated to molybdenum. Structural data complemented with EPR studies on alcohol-inhibited *Dg*AOR show that the nearly square pyramidal coordination of the as-purified enzyme is distorted on inhibition. This process involves the loss of the OH_x ligand and the binding to the Mo atom of the alcohol molecule in a η^2 fashion, which is accompanied with changes in the electronic structure of the Mo site, favoring a larger magnetic coupling with the proximal FeS center. The most noticeable

(53) Bencini, A.; Gatteschi, D. *Electron Paramagnetic Resonance of Exchange Coupled Systems*; Springer-Verlag: Berlin, 1990.

(54) Palanca, P.; Picher, T.; Sanz, V.; Gomez-Romero, P.; Llopis, E.; Domenech, A.; Cervill, A. *J. Chem. Soc., Chem. Commun.* **1990**, 531–533.

(55) Brew, S. A.; Dossett, S. J.; Jeffery, J. C.; Stone, F. G. A. *J. Chem. Soc., Dalton Trans.* **1990**, 3709–3718.

(56) Brookhart, M.; Green, M. L.; Parkin, G. *Proc. Natl. Acad. Sci. U.S.A.* **2007**, *104*, 6908–6914.

characteristic of the Mo−alcohol adduct is the formation of a direct bond between the molybdenum and one of the carbon atoms of the alcohol moiety, which constitutes the first direct evidence for such a bond in a biological system. Because of the competitive character of these inhibitors, changes in the coordination sphere of the molybdenum upon inhibition might be related to those occurring during catalysis, which is the subject of ongoing investigation.

Acknowledgment. T.S.S and P.J.G thank Fundação para a Ciência e Tecnologia for funding (Grants SFRH/BPD/26991/2006 and SFRH/BPD/29812/2006, respectively). C.D.B. and J.J.G.M. thank SECYT (Argentina) and GRICES (Portugal) for a bilateral collaborative grant. Work was supported by projects PTDC/QUI/64733/2006 and POCTI/1999/BME/36152, POCTI/QUI/57641/2004 in Portugal and SEPCyT:PICT 2006-00439, CONICET PIP 02559/2000, and CAI+D-UNL in Argentina. C.D.B is a member of CONICET (Argentina).

Supporting Information Available: Steady-state kinetic plots used to determine kinetic parameters and inhibition patterns of cyanide, ethylene glycol, and glycerol and rmsd values for the superposition of AOR crystal structures. This material is available free of charge via the Internet at http://pubs.acs.org.

JA809448R